

**Bright solitons in nonlinear media with a self-defocusing double-well nonlinearity**Qiongtao Xie,<sup>1,2,\*</sup> Linmao Wang,<sup>1</sup> Yizhen Wang,<sup>1</sup> Zhenjiang Shen,<sup>1</sup> and Jun Fu<sup>1</sup><sup>1</sup>*College of Physics and Electronic Engineering, Hainan Normal University, Haikou 571158, China*<sup>2</sup>*Department of Physics, Hunan Normal University, Changsha 410081, China*

(Received 18 August 2014; revised manuscript received 21 October 2014; published 29 December 2014)

We show that stable bright solitons can appear in a medium with spatially inhomogeneous self-defocusing (SDF) nonlinearity of a double-well structure. For a specific choice of the nonlinearity parameters, we obtain exact analytical solutions for the fundamental bright solitons. By making use of the linear stability analysis, the stability region in the parameter space for the exact fundamental bright soliton is obtained numerically. We also show the bifurcation from an antisymmetric to an asymmetric bright soliton for the SDF double-well nonlinearity.

DOI: [10.1103/PhysRevE.90.063204](https://doi.org/10.1103/PhysRevE.90.063204)

PACS number(s): 05.45.Yv, 42.65.Tg, 42.65.Jx, 42.65.Wi

**I. INTRODUCTION**

Solitons are important nonlinear waves and appear in various physical systems, such as Bose-Einstein condensate (BEC) [1–4] and optical systems [5,6]. In certain situations for these systems, a nonlinear Schrödinger equation (NLSE) provides a fundamental model for investigating the properties of solitons. It is well-known that, in NLSEs with spatially homogeneous nonlinearity and no linear external potentials, self-focusing (SF) and self-defocusing (SDF) nonlinearities support bright and dark solitons, respectively.

Recently, solitons in nonlinear media with spatially inhomogeneous nonlinearity have attracted extensive interest [7]. In comparison with uniform nonlinearity, nonuniform nonlinearity may lead to many novel and interesting effects. For example, in nonlinear lattices where nonlinearity varies periodically in space, solitons may exist with an arbitrarily small value of the norm [8]. If the modulation strength for nonlinear lattices is strong enough, all Bloch waves become dynamically unstable [9]. In addition, it has been shown that nonuniform nonlinearity can strongly modify the condition for the existence of solitons. It has been found that in nonuniform conservative systems a purely SDF nonlinearity can support stable bright solitons [10,11]. The formation of stable bright solitons requires diverging nonlinearities. Several different types of such nonlinearities have been discussed [10–22]. In certain situations, exact analytical results for bright soliton solutions have been obtained. In most of these previous works, spatially inhomogeneous SDF nonlinearities display a single-well structure, including anti-Gaussian [10,12,15,17,18], exponential [10,14,20–22], and algebraic [11,16,22] nonlinearities.

In this article, we consider a type of spatially inhomogeneous SDF nonlinearity with a double-well structure. The SDF double-well nonlinearity provides a previously unexplored setting where solitons can be studied. It is shown that stable bright solitons can appear in such a SDF double-well nonlinearity. In particular, it is found that, for a specific choice of the nonlinearity parameters, exact analytical solutions for fundamental bright solitons can be obtained. With the linear stability analysis, we present the boundary between the stable and unstable region in the parameter plane for the exact

fundamental bright soliton. In addition, we show that beyond a critical norm, antisymmetric solitons with one node become asymmetric. This effect is related to the bifurcation from an antisymmetric to an asymmetric soliton.

**II. BRIGHT SOLITONS IN A SELF-DEFOCUSING DOUBLE-WELL NONLINEARITY**

We consider the nonlinear optical system where the light is propagating along the  $z$  direction and strongly localized in the  $y$  direction. The light propagation in the nonlinear media is thus described by the NLSE [5–7]

$$i \frac{\partial \psi}{\partial z} = -\frac{\partial^2 \psi}{\partial x^2} + g(x)|\psi|^2 \psi, \quad (1)$$

where  $\psi(x, z)$  is the scaled field amplitude and  $g(x)$  is the nonlinear refractive index profile along the  $x$  direction. In optical systems, one can use inhomogeneous doping to create such nonlinearity modulation [23,24]. In BEC systems, the spatially inhomogeneous nonlinearity may be generated by using the Feshbach resonance with properly chosen external fields [25,26]. The soliton solutions to Eq. (1) are written as  $\psi(x, z) = \phi(x) \exp(ibz)$ , where  $b$  is the propagation constant and  $\phi(x)$  is the real function satisfying the following equation:

$$b\phi - \frac{d^2\phi}{dx^2} + g(x)\phi^3 = 0. \quad (2)$$

In the present study, we mainly focus on a three-parameter family of the nonlinearities

$$g(x) = g_0 + g_1 \operatorname{sech}^2(x) + g_2 \cosh^2(x). \quad (3)$$

After a simple calculation, one can find that under the conditions of  $g_{1,2} > 0$ ,  $g_1/g_2 > 1$ , and  $2\sqrt{g_1 g_2} + g_0 \geq 0$ , the nonlinearity  $g(x) \geq 0$  displays two local minima at  $x_{\pm} = \pm \operatorname{arccosh}((g_1/g_2)^{1/4})$ . If the conditions of  $g_{1,2} > 0$ ,  $g_1/g_2 \leq 1$ , and  $g_0 + g_1 + g_2 \geq 0$  are satisfied, the nonlinearity  $g(x) \geq 0$  has one minimum at  $x = 0$ . In the following, we show that for certain specific values of  $g_{0,1,2}$ , the exact analytical solution for the fundamental bright solitons to Eq. (2) can be obtained in an explicit form.

It is found that for the special forms of  $g_{0,1,2}$

$$g_0^{\text{ex}} = 2\eta(\kappa - 4 - \eta), \quad g_1^{\text{ex}} = 6\eta + \kappa, \quad g_2^{\text{ex}} = \kappa\eta^2, \quad (4)$$

\*qiongtaoxie@yahoo.com

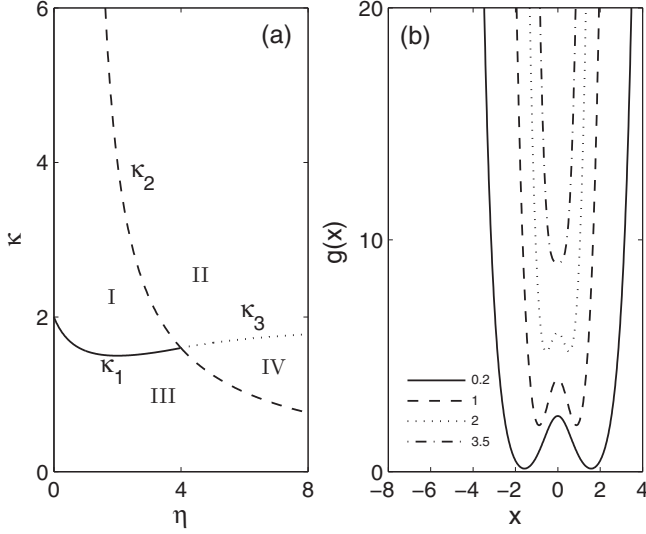


FIG. 1. (a) Four parameter regions for the nonlinearity  $g(x)$  in the plane  $(\kappa, \eta)$ . Here  $\kappa_1 = (\eta + 4)^2/8(1 + \eta)$  with  $0 < \eta \leq 4$  (solid line),  $\kappa_2 = 6\eta/(\eta^2 - 1)$  with  $\eta > 1$  (dashed line), and  $\kappa_3 = 2\eta/(1 + \eta)$  with  $\eta \geq 4$  (dotted line). In the I region,  $g(x) > 0$  displays two local minima at  $x_{\pm} = \pm \text{arccosh}[(6\eta + \kappa)^{1/4}/(\kappa\eta^2)^{1/4}]$ , and in the II region,  $g(x) > 0$  displays a single minimum at  $x = 0$ . (b) Profiles of the nonlinearity  $g(x)$  with  $\kappa = 2$  for different values of  $\eta$ .

Eq. (2) admits the exact solution for fundamental bright solitons:

$$\phi_{\text{ex}}(x) = \frac{\cosh(x)}{1 + \eta \cosh^2(x)}, \quad (5)$$

with the propagation constant

$$b_{\text{ex}} = 1 - \kappa. \quad (6)$$

Here  $\eta > 0$  and  $\kappa > 0$  are two new parameters. For the set of specially chosen parameters (4), we have four different regions in the parameter plane  $(\kappa, \eta)$ , denoted by I–IV in Fig. 1(a). The boundary lines between the four regions are determined by the three curves,  $\kappa_1 = (\eta + 4)^2/8(1 + \eta)$  with  $0 < \eta \leq 4$  (solid line),  $\kappa_2 = 6\eta/(\eta^2 - 1)$  with  $\eta > 1$  (dashed line), and  $\kappa_3 = 2\eta/(1 + \eta)$  with  $\eta \geq 4$  (dotted line). At  $\eta = 4$ , we have  $\kappa_1 = \kappa_2 = \kappa_3$ . In the I region,  $g(x) > 0$  displays two local minima at  $x_{\pm} = \pm \text{arccosh}\{[(6\eta + \kappa)/\kappa\eta^2]^{1/4}\}$ , and in the III region,  $g(x)$  also has two local minima at  $x_{\pm}$  but with  $g(x_{\pm}) < 0$ . In the II region,  $g(x) > 0$  displays a single minimum at  $x = 0$ , and in the IV region,  $g(x)$  has a single minimum at  $x = 0$  with  $g(0) < 0$ . In Fig. 1(b), we show the profiles of the nonlinearity  $g(x)$  with a fixed value of  $\kappa = 2$  for different values of  $\eta$ . It is seen that as  $\eta$  is increased,  $g(x)$  undergoes a transition from the I region to the II region, and thus varies from double well to single well.

An important issue is the stability of the exact solutions. The stability can be analyzed with the linear stability analysis. We may perturb them as  $\psi(x, z) = \exp(ibz)\{\phi(x) + [v(x) - w(x)]\exp(\varepsilon z) + [v^*(x) + w^*(x)]\exp(\varepsilon^* z)\}$  [27], where  $|v|, |w| \ll 1$ . Upon substituting this expansion into Eq. (1) and linearizing it, we obtain the linear stability eigenvalue

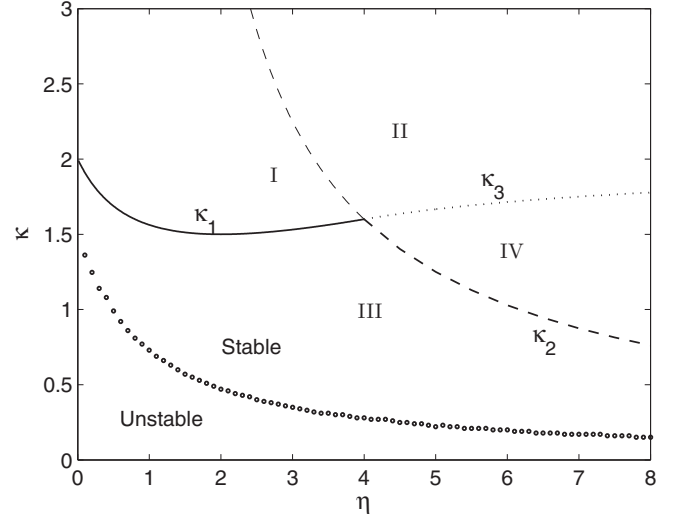


FIG. 2. Boundary line, marked by the circles, between the stable and unstable exact bright solitons in the parameter space  $(\kappa, \eta)$ .

problem for perturbation growth rates  $\varepsilon$  [27]:

$$\begin{aligned} -i \left( \frac{d^2}{dx^2} - b - g\phi^2 \right) w &= \varepsilon v, \\ -i \left( \frac{d^2}{dx^2} - b - 3g\phi^2 \right) v &= \varepsilon w. \end{aligned} \quad (7)$$

The exact soliton solution is linearly stable if and only if there are no eigenvalues  $\varepsilon$  with a positive real part. We may compute numerically the eigenvalues by using the Fourier collocation method [27]. With linear stability analysis, we can numerically find the boundary line for the stable and unstable exact bright solitons. In Fig. 2, the circles are for the numerical results for the boundary line in the parameter plane  $(\kappa, \eta)$ . It is observed that the exact fundamental bright soliton is stable in both the I and II regions.

Now we give a brief discussion about the properties of the exact bright soliton. In the range of  $0 < \eta < 1$ , the exact bright soliton  $\phi_{\text{ex}}(x)$  displays two peaks at  $x_{\pm}^p = \pm \text{arccosh}[(1/\eta)^{1/2}]$ , and in the range of  $\eta \geq 1$ , it displays a single peak at  $x = 0$ . The propagation constant  $b_{\text{ex}}$  for the exact solution is less than zero,  $b_{\text{ex}} = 1 - \kappa < 0$ , in the I and II regions with  $\kappa > 1$ . The obtained fundamental bright soliton has the asymptotical behavior  $\phi_{\text{ex}}(x) \rightarrow \text{sech}(x)$  as  $x \rightarrow \pm\infty$ . For families of fundamental bright solitons for the SDF nonlinearity  $g(x) > 0$ , these results can also be understood with the Thomas-Fermi (TF) approximation which neglects the diffraction term in Eq. (2) [11]. This approximation leads to the explicit expression for the spatial shape of the fundamental solitons:

$$\phi_{\text{TF}}(x) = \frac{\sqrt{-b}}{\sqrt{g_0 + g_1 \text{sech}^2(x) + g_2 \cosh^2(x)}}. \quad (8)$$

This result tells us that the fundamental bright solitons exist for  $b < 0$  and vary as  $\phi_{\text{TF}}(x) \rightarrow \text{sech}(x)$  as  $x \rightarrow \pm\infty$ .

If the parameters  $g_{0,1,2}$  and  $b$  are different from those in Eqs. (4) and (6), exact solutions for bright solitons are not available at present. In principle, one can use the numerical

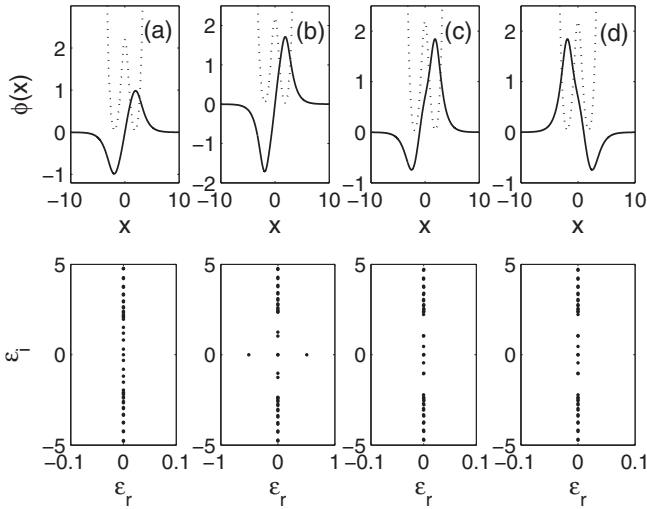


FIG. 3. (a)–(d) Profiles of the antisymmetric and asymmetric solitons for fixed values of  $\eta = 0.1$  and  $\kappa = 2$ . In panel (a),  $b = -0.8$ , and in panels (b)–(d),  $b = -1.2$ . The bottom panels are the linear stability for panels (a)–(d). In panels (a)–(d), the dotted lines denote the double-well nonlinearities  $g(x) > 0$ .

methods to find various types of solitons. In Figs. 3(a)–3(d), we show the profiles of the bright solitons with one node for two different values of  $b = -0.8$  and  $b = -1.2$  with fixed values of  $\eta = 0.1$  and  $\kappa = 2$ . Their stability is given in the bottom panels of Fig. 3, where  $\epsilon_r$  and  $\epsilon_i$  are the real and imaginary parts of  $\epsilon$ . In the case of  $b = -0.8$ , the antisymmetric bright soliton is stable. In the case of  $b = -1.2$ , the corresponding antisymmetric bright soliton is unstable, and a stable asymmetric bright soliton appears. To quantify the asymmetry of these asymmetric solitons, we define the population imbalance in the nonlinear double wells as

$$\Theta = \frac{\int_{-\infty}^0 \phi^2(x) dx - \int_0^{\infty} \phi^2(x) dx}{\int_{-\infty}^{\infty} \phi^2 dx}, \quad (9)$$

where  $U = \int_{-\infty}^{\infty} \phi^2 dx$  is the norm of the soliton. In Fig. 4, we display the population imbalance  $\Theta$  and norm  $U$  as a function of  $b$  for the antisymmetric solitons with one node. It is found that there is a symmetry breaking (pitchfork bifurcation) for the antisymmetric bright soliton [28]. As  $b$  is decreased below a certain critical value of  $b_c \approx -0.84$ , the stable asymmetric solitons appear, while the originally stable antisymmetric bright solitons become unstable. The critical value  $b_c$  is related to the critical value  $U_c \approx 4.65$ . For the fundamental bright solitons, the symmetry breaking does not happen.

Our results can also be illustrated by direct numerical simulations of Eq. (1) by making use of the operator-splitting method. In Fig. 5, we show the stable and unstable propagation of the exact fundamental solitons for two sets of parameters, respectively. The first set of parameters is chosen as  $\eta = 0.1$  and  $\kappa = 2$  in the stable I region. The second set of parameters is given as  $\eta = 0.1$  and  $\kappa = 1.1$  in the unstable space of the III region. It is found that the unstable soliton evolves into the asymmetric state. This is possibly due to the presence of stable asymmetric solitons, as shown in Figs. 6(b) and 6(c).

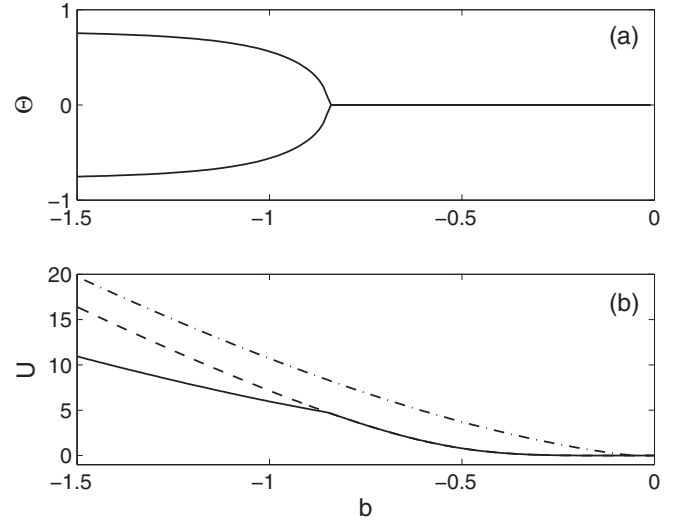


FIG. 4. (a) The population imbalance  $\Theta$  of the antisymmetric and asymmetric bright solitons with one node as a function of  $b$  with  $\eta = 0.1$  and  $\kappa = 2$ . (b) The norm of the bright solitons as a function of  $b$ . In panel (b), the dashed line denotes the unstable antisymmetric bright solitons, and the dashed-dotted line is for the fundamental bright solitons.

The unstable fundamental bright soliton is driven near certain one branch of the asymmetric solitons under the action of the noise. We note that for the second set of parameters, we have  $g(x) < 0$  in certain small regions, as shown in Fig. 6. This means that although the SDF nonlinearity is dominant, the fundamental bright solitons undergo a bifurcation under certain conditions. This issue shall be discussed in detail in a future study.

In our previous discussions, the SDF double-well nonlinearity  $g(x)$  in Eq. (3) is of the exponential shape. In fact, there exist other forms of the nonlinearities  $g(x)$  with a double-well structure which support exact bright soliton solutions. For

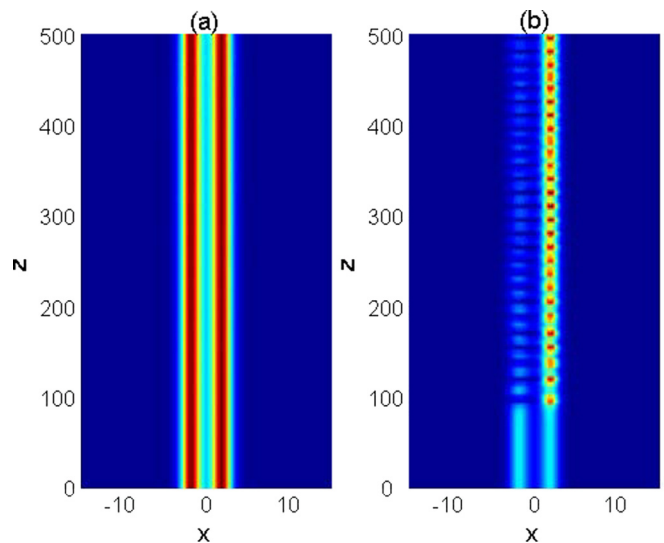


FIG. 5. (Color online) A contour plot of  $|\psi(x, z)|^2$  demonstrating the stable and unstable propagation of the exact fundamental bright soliton. In panel (a),  $\eta = 0.1$  and  $\kappa = 2$ , and in panel (b),  $\eta = 0.1$  and  $\kappa = 1.1$ .

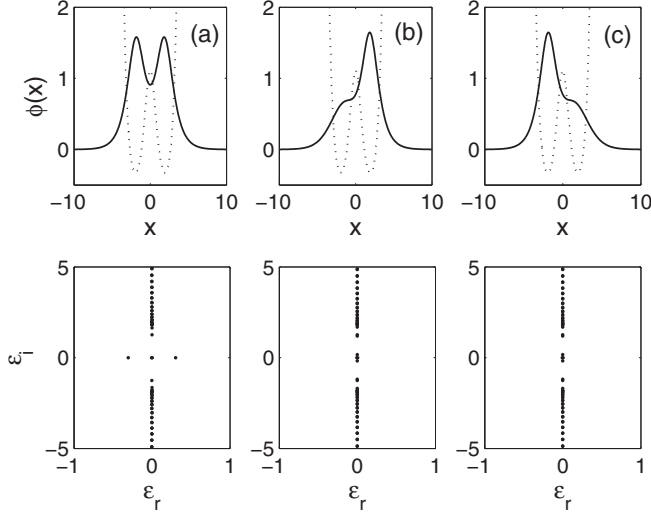


FIG. 6. (a)–(c) Profiles of the fundamental solitons for fixed values of  $\eta = 0.1$ ,  $\kappa = 1.1$ , and  $b = 1 - \kappa = -0.1$ . The bottom panel is the linear stability of panels (a)–(c). In panels (a)–(c), the dotted lines show the double-well nonlinearities.

example, if the nonlinearity has the anti-Gaussian form,

$$g(x) = \left( \frac{4\kappa^2/\eta}{(1+\eta x^2)} - \frac{4\kappa^2/\eta}{(1+\eta x^2)^2} + \frac{8\kappa+2\eta}{(1+\eta x^2)^3} \right) e^{2\kappa x^2}, \quad (10)$$

exact solution for the fundamental bright solitons is available:

$$\phi(x) = e^{-\kappa x^2} (1 + \eta x^2), \quad (11)$$

with  $b = -10\kappa$ . Under certain parameter conditions, for example,  $\eta > \kappa > 0$ ,  $g(x) > 0$  shows a double-well structure, and  $\phi(x)$  has two peaks. For the algebraic nonlinearity

$$g(x) = g_0 + \frac{g_1}{1+\eta x^2} + \frac{g_2}{(1+\eta x^2)^2} + \frac{g_3}{(1+\eta x^2)^3} + g_4 x^2, \quad (12)$$

with

$$\begin{aligned} g_0 &= \kappa \frac{\eta_2^2}{\eta_1^2} + 2 \frac{\eta_2^2}{\eta_1} + 2\kappa \frac{\eta_2}{\eta_1} \left( 1 - \frac{\eta_2}{\eta_1} \right), \\ g_1 &= \frac{\eta_2}{\eta_1} (3\eta_2 - 6\eta_1), \quad g_2 = 6 \frac{\eta_2}{\eta_1} (\eta_1 - \eta_2), \\ g_3 &= 6 \frac{\eta_2}{\eta_1} + \eta_1 - 2\eta_2, \quad g_4 = \kappa \frac{\eta_2^2}{\eta_1}, \end{aligned}$$

we may obtain an exact solution for the fundamental bright solitons:

$$\phi(x) = \frac{\sqrt{1 + \eta_1 x^2}}{1 + \eta_2 x^2}, \quad (13)$$

with  $b = -\kappa$ . Under certain conditions,  $g(x) > 0$  is of a double-well structure, and  $\phi(x)$  has two peaks.

### III. CONCLUSION

In conclusion, we have shown that stable bright solitons can exist in spatially inhomogeneous SDF nonlinearity with a double-well structure. Under certain special conditions of the nonlinearity parameters, we have presented an exact analytical solution for fundamental bright solitons. The stability of the exact fundamental bright solitons is analyzed numerically by means of linear stability analysis and direct numerical simulation. In addition, it is found that the bifurcation of antisymmetric solitons occurs, but is absent for fundamental solitons.

### ACKNOWLEDGMENTS

The authors thank Yongping Zhang for many helpful discussions. This work is supported by the National Natural Science Foundation of China under Grants No. 11375059 and No. 11304069 and by the Scientific Research Fund of Hunan Provincial Education Department under Grant No. 13A058.

- 
- [1] L. Khaykovich, F. Schreck, G. Ferrari, T. Bourdel, J. Cubizolles, L. D. Carr, Y. Castin, and C. Salomon, *Science* **296**, 1290 (2002).
  - [2] K. E. Strecker, G. B. Partridge, A. G. Truscott, and R. G. Hulet, *Nature (London)* **417**, 150 (2002).
  - [3] S. Burger, K. Bongs, S. Dettmer, W. Ertmer, K. Sengstock, A. Sanpera, G. V. Shlyapnikov, and M. Lewenstein, *Phys. Rev. Lett.* **83**, 5198 (1999).
  - [4] J. Denschlag, J. E. Simsarian, D. L. Feder, Charles W. Clark, L. A. Collins, J. Cubizolles, L. Deng, E. W. Hagley, K. Helmerson, W. P. Reinhardt, S. L. Rolston, B. I. Schneider, and W. D. Phillips, *Science* **287**, 97 (2000).
  - [5] Y. S. Kivshar and G. Agrawal, *Optical Solitons: From Fibers to Photonic Crystals* (Academic Press, San Diego, 2003).
  - [6] Z. Chen, M. Segev, and D. N. Christodoulides, *Rep. Prog. Phys.* **75**, 086401 (2012).
  - [7] Y. V. Kartashov, B. A. Malomed, and L. Torner, *Rev. Mod. Phys.* **83**, 247 (2011).
  - [8] H. Sakaguchi and B. A. Malomed, *Phys. Rev. E* **72**, 046610 (2005).
  - [9] S.-L. Zhang, Z.-W. Zhou, and B. Wu, *Phys. Rev. A* **87**, 013633 (2013).
  - [10] O. V. Borovkova, Y. V. Kartashov, L. Torner, and B. A. Malomed, *Phys. Rev. E* **84**, 035602(R) (2011).
  - [11] O. V. Borovkova, Y. V. Kartashov, B. A. Malomed, and L. Torner, *Opt. Lett.* **36**, 3088 (2011).
  - [12] W.-P. Zhong, M. Belić, G. Assanto, B. A. Malomed, and T. Huang, *Phys. Rev. A* **84**, 043801 (2011).
  - [13] Q. Tian, L. Wu, Y. Zhang, and J.-F. Zhang, *Phys. Rev. E* **85**, 056603 (2012).
  - [14] V. E. Lobanov, O. V. Borovkova, Y. V. Kartashov, B. A. Malomed, and L. Torner, *Opt. Lett.* **37**, 1799 (2012).
  - [15] Y. V. Kartashov, V. E. Lobanov, B. A. Malomed, and L. Torner, *Opt. Lett.* **37**, 5000 (2012).

- [16] Y. Wu, Q. Xie, H. Zhong, L. Wen, and W. Hai, *Phys. Rev. A* **87**, 055801 (2013).
- [17] R. Driben, Y. V. Kartashov, B. A. Malomed, T. Meier, and L. Torner, *Phys. Rev. Lett.* **112**, 020404 (2014).
- [18] Y. V. Kartashov, V. A. Vysloukh, L. Torner, and B. A. Malomed, *Opt. Lett.* **36**, 4587 (2011).
- [19] O. V. Borovkova, Y. V. Kartashov, V. A. Vysloukh, V. E. Lobanov, B. A. Malomed, and L. Torner, *Opt. Express* **20**, 2657 (2012).
- [20] J. Zeng and B. A. Malomed, *Phys. Rev. E* **86**, 036607 (2012).
- [21] Y. He and B. A. Malomed, *Phys. Rev. A* **87**, 053812 (2013).
- [22] W. B. Cardoso, J. Zeng, A. T. Avelar, D. Bazeia, and B. A. Malomed, *Phys. Rev. E* **88**, 025201 (2013).
- [23] J. Hukriede, D. Runde, and D. Kip, *J. Phys. D: Appl. Phys.* **36**, R1 (2003).
- [24] K. Peithmann, J. Hukriede, K. Buse, and E. Krätzig, *Phys. Rev. B* **61**, 4615 (2000).
- [25] G. Roati, M. Zaccanti, C. D'Errico, J. Catani, M. Modugno, A. Simoni, M. Inguscio, and G. Modugno, *Phys. Rev. Lett.* **99**, 010403 (2007).
- [26] S. E. Pollack, D. Dries, M. Junker, Y. P. Chen, T. A. Corcovilos, and R. G. Hulet, *Phys. Rev. Lett.* **102**, 090402 (2009).
- [27] J. Yang, *J. Comp. Phys.* **227**, 6862 (2008).
- [28] G. Theocharis, P. G. Kevrekidis, D. J. Frantzeskakis, and P. Schmelcher, *Phys. Rev. E* **74**, 056608 (2006).